

Astro2020 Science White Paper

Mapping Cosmic Dawn and Reionization: Challenges and Synergies

Thematic Areas:

- ☐ Planetary Systems ☐ Star and Planet Formation
☐ Formation and Evolution of Compact Objects ☒ Cosmology and Fundamental Physics
☐ Stars and Stellar Evolution ☐ Resolved Stellar Populations and their Environments
☒ Galaxy Evolution ☐ Multi-Messenger Astronomy and Astrophysics

Principal Authors:

Marcelo A. Alvarez¹, Anastasia Fialkov², Paul La Plante³

Co-authors:

James Aguirre, Yacine Ali-Haïmoud, George Becker, Judd Bowman, Patrick Breysse, Volker Bromm, Philip Bull, Jack Burns, Nico Cappelluti, Isabella Carucci, Tzu-Ching Chang, Kieran Cleary, Asantha Cooray, Xuelei Chen, Hsin Chiang, Joanne Cohn, David DeBoer, Joshua Dillon, Olivier Doré, Cora Dvorkin, Simone Ferraro, Steven Furlanetto, Bryna Hazelton, J. Colin Hill, Daniel Jacobs, Kirit Karkare, Garrett K. Keating, Léon Koopmans, Ely Kovetz, Adam Lidz, Adrian Liu, Yin-Zhe Ma, Yi Mao, Kiyoshi Masui, Matthew McQuinn, Jordan Mirocha, Julian Muñoz, Steven Murray, Aaron Parsons, Jonathan Pober, Benjamin Saliwanchik, Jonathan Sievers, Nithyanandan Thyagarajan, Hy Trac, Alexey Vikhlinin, Eli Visbal, Matias Zaldarriaga

Abstract:

Cosmic dawn and the Epoch of Reionization (EoR) are among the least explored observational eras in cosmology: a time at which the first galaxies and supermassive black holes formed and reionized the cold, neutral Universe of the post-recombination era. With current instruments, only a handful of the brightest galaxies and quasars from that time are detectable as individual objects, due to their extreme distances. Fortunately, a multitude of multi-wavelength intensity mapping measurements, ranging from the redshifted 21 cm background in the radio to the unresolved X-ray background, contain a plethora of synergistic information about this elusive era. The coming decade will likely see direct detections of inhomogeneous reionization with CMB and 21 cm observations, and a slew of other probes covering overlapping areas and complementary physical processes will provide crucial additional information and cross-validation. To maximize scientific discovery and return on investment, coordinated survey planning and joint data analysis should be a high priority, closely coupled to computational models and theoretical predictions.

¹University of California, Berkeley; marcelo.alvarez@berkeley.edu

²University of Sussex; a.fialkov@sussex.ac.uk

³University of Pennsylvania; plaplant@sas.upenn.edu

The High-redshift Frontier

The epochs of cosmic dawn and reionization are filled with opportunity for exploring cosmological evolution. Thus far, sensitive ground and space based instruments – covering a wide range of the electromagnetic spectrum – have been used to detect, study, and catalog individual objects well into the EoR, out to redshifts as high as $z \sim 10$ (Bouwens et al., 2015; Venemans et al., 2017; Bosman et al., 2018). However, the bright objects studied with these instruments are not a representative sample. Without alternative probes of this elusive chapter of cosmic history, significant gaps will remain.

Fortunately a complementary approach exists, focused on nearly uniform surveys of large regions of the sky over a broad range of wavelengths to obtain maps of the combined emission, scattering and absorption from the stars, black holes, dust, and gas that existed in the early universe. Such maps represent an unbiased sample of all the photons available over the wavelengths and areas surveyed, and contain valuable information even if all the discrete sources are confusion-limited, the value at each pixel is noise-dominated, or both. A wide variety of map-based analysis techniques, many of which have already been developed to study diffuse Galactic structure and the cosmic microwave background (CMB), are available to extract the relevant information.

In this white paper, we describe the promise and challenges of multi-wavelength mapping of the high redshift universe in the coming decade. We argue that the planned and proposed high-redshift surveys are highly synergistic – the amount of mutual information contained in data obtained using instruments with very different systematic effects allows cross-validation of detections and highlights information that is not apparently manifested in each individual tracer. This synergistic approach might also be beneficial when extracting weak signals hidden under strong foregrounds and systematics. Studying the aggregate effects of the complex processes comes with unique and significant challenges, both for astrophysical modeling in an era about which we know very little, as well as for the mitigation of foreground contamination and instrumental systematics. Consequently, significant coordination between the various experiments that will gather the data used to produce these maps is crucial, from instrument design, to survey strategy, and finally joint analysis and cross-correlation.

Intensity Mapping from the Radio to X-ray

The redshifted 21 cm background from the hyperfine transition of hydrogen is a probe of the neutral intergalactic medium (IGM) and the history of its heating and reionization, while secondary CMB anisotropies and spectral distortions from Thomson scattering by electrons during reionization are sensitive to its overall morphology and history. Line intensity mapping of various molecular and atomic lines can be used to characterize properties of first stars and galaxies, and the unresolved X-ray background contains information on the abundance and properties of energetic high-redshift sources such as accreting black holes, supernovae, and X-ray binaries.

Redshifted 21 cm Background

The 21 cm signal is produced by neutral hydrogen atoms in the medium outside the star forming regions. The intensity and spatial fluctuations of this signal depend on the ultraviolet and X-ray radiative backgrounds produced by the first stars, galaxies, and black holes. Therefore, the signal can be used as a probe of the early star and black hole formation. 21 cm cosmology is on the brink of a revolution: the EDGES Low-Band collaboration has claimed the first detection

of an absorption feature from redshift $z \sim 17$ (yet to be confirmed, Bowman et al. 2018), and pioneering global-signal experiments have ruled out physically motivated models based on results from $6 \lesssim z \lesssim 15$ (Monsalve et al., 2017, 2018; Singh et al., 2017, 2018). Despite the large variety of plausible theoretical scenarios (e.g., Cohen et al. 2017), the first claimed detection does not comply with standard astrophysical predictions.

Beyond this pioneering effort, the international community is heavily committed to observations of the correlated spatial fluctuations in the power spectrum of the 21 cm signal with facilities such as: the Low Frequency Array (LOFAR), which yielded upper limits on the 21 cm power spectrum at $z \sim 10$ (Patil et al., 2017) and $20 \lesssim z \lesssim 25$ (Gehlot et al., 2018); the Hydrogen Epoch of Reionization Array (HERA, DeBoer et al. 2017), which is projected to be fully constructed in late 2019; space-based missions such as DAPPER (Burns et al., 2018); and the future Square Kilometre Array (SKA), whose Phase-1 observation is expected to yield initial scientific results around 2023. These power spectrum measurements can provide important results for testing the reality of results from global signal measurements like EDGES (Fialkov & Barkana, 2019).

Cosmic Microwave Background

The “patchy” spatial distribution of electrons that result from what is very likely to be a highly inhomogeneous reionization process is imprinted with high fidelity through Thomson scattering of primary CMB photons. The kinetic Sunyaev-Zel’dovich (kSZ) effect is a secondary temperature anisotropy in the CMB that is caused by the motion of electrons relative to the CMB rest frame and interacting with CMB photons via Thomson scattering. The high- z kSZ signal arises primarily by the same patchy ionization field that generates the redshifted 21 cm background fluctuations, so the CMB temperature and redshifted 21 cm background should therefore be correlated. The magnitude and scale dependence of the kSZ power spectrum are sensitive to the overall reionization history and morphology. For example, the duration of the EoR affects the magnitude of the kSZ signal, with longer epochs leading to larger kSZ signals.

Additionally, CMB secondary temperature and polarization anisotropies are created by a modulation of primary temperature and polarization fluctuations due to line of sight fluctuations in the optical depth (“screening”; Dvorkin & Smith 2009; Dvorkin et al. 2009) or the generation of additional linear polarization in response to the local quadrupolar anisotropy seen by electrons during reionization (“scattering”; Mortonson & Hu 2008). In Dvorkin & Smith (2009), a statistical technique for extracting the inhomogeneous reionization signal from high-sensitivity measurements of the CMB temperature and polarization fields was proposed. Recent work shows this signal may be detectable by CMB-S4 through the B-mode power at $50 \lesssim \ell \lesssim 500$ or by explicit reconstruction of the optical depth at the map level (Roy et al., 2018).

Line Intensity Mapping (LIM)

Characterizing properties of typical star forming high-redshift galaxies requires measurements of molecular gas in objects which are below the detection threshold of current telescopes. Molecular and atomic emission lines from dusty high-redshift galaxies could be strong enough to allow intensity mapping (IM) of this signal (for a recent review see Kovetz et al. 2017). The amplitude of the CO power spectrum was recently tentatively detected in the shot noise regime by an intensity mapping experiment, the CO Power Spectrum Survey (COPSS, Keating et al., 2016). This experiment measured the power spectrum of CO for the J_{1-0} transition with a rest-frame frequency of 115.27 GHz from galaxies in the redshift range $2.3 < z < 3.3$, an important proof-

of-concept for line intensity mapping of galaxies using CO. The CO Mapping Array Pathfinder (COMAP, Cleary et al. 2016) experiment is currently underway and aims to constrain the CO clustering power spectrum from galaxies at $2.4 < z < 3.4$ in this first phase and at $6 < z < 8$ in a future phase.

Metal fine structure lines probe gas in various environments and provide information about star formation rates in galaxies. For example [OIII] emission is relatively easy to model because it originates primarily from ionized regions and was recently detected by ALMA at $7 \lesssim z \lesssim 9$, with the most distant object located at $z = 9.11$ (Hashimoto et al., 2018). Moriwaki et al. (2018) used high-resolution simulations to study [OIII] emission from galaxies at $z > 7$ and suggest that systematic surveys with JWST NIRCarn can also probe the large-scale structure at $z > 8$. The TIME-Pilot (Crites et al., 2014), CONCERTO (Lagache, 2017), and CCAT-prime (Parshley et al., 2018) experiments are specifically designed to observe [CII] emission lines from the EoR and the post-reionization epoch. CDIM (Cooray et al., 2016) is a proposed satellite experiment that will map the Ly α sky from redshifts $6 < z < 8$, and will contain valuable information about the IGM from the EoR. The Ly α forest contains clues to the detailed ionization and thermal state of the gas in the IGM, especially from times post-reionization.

Unresolved X-ray Background

Detection of X-ray emission from high redshifts could constrain formation of super-massive black holes and properties of the first population of X-ray binaries. Direct observations of high- z populations require large integration times and can detect only the brightest objects at high redshifts, while fainter and more common high- z sources are undetectable individually. As a result, the observed objects are not a good statistical sample of the population, and the clustering information is lost. A useful measurement is that of the unresolved cosmic X-ray background (CXB) in the soft band (0.5-2 keV) reported by the *Chandra* X-ray observatory, which constrains both the luminosity and clustering of the most common objects. Evidences and constraints on the X-rays emerging from the EoR and observed in the CXB have been presented by Lehmer et al. (2012), Cappelluti et al. (2012, 2013), and Mitchell-Wynne et al. (2016). However, the origin of this cross-power is uncertain. Future facilities will improve the situation. A US-led *Lynx* mission concept will have a somewhat smaller field of view but much higher angular resolution and sensitivity. *Lynx* will be able to reach into extremely low flux levels ($\sim 1/100$ of *Chandra*) without being affected by source confusion. As a result, the residual background fluctuations due to undetected intrinsically faint $1 < z < 3$ objects are an order of magnitude lower for *Lynx* than for *Athena* (The *Lynx* Team, 2018).

Synergies between Probes

High-redshift astrophysical processes should imprint consistent signatures that naturally lead to correlations between the 21 cm signal, unresolved X-ray background (Fialkov et al., 2017; Ma et al., 2018a), intensity mapping of atomic and molecular lines, and number counts of high-redshift galaxies. Although each of the probes discussed above provide important constraints on their own, their use in cross-correlation with the results from other probes can yield additional scientific insight. To enable synergies, coordinated surveys of the same part of the sky with different instruments is necessary. Measurements made from using cross-correlations potentially have a larger *noise* than the auto-correlations, but are not *biased*. They are also expected to be less sensitive to systematic errors.

CMB-21cm

The 21 cm and kSZ signals should be non-vanishing when computing the cross-correlation between them in map space. Because the kSZ signal can be positive or negative (depending on whether the peculiar velocity of the distant galaxies are toward or away from Earth), the simple cross-correlation signal suffers from severe cancellation. One way forward is to perform cross-correlations between the absolute value of the kSZ field, or the value of the kSZ field squared (Ma et al., 2018b). Alternatively, by computing a higher-point statistic such as the bispectrum between two maps of the kSZ field and one map of the T21 field, this cancellation can be avoided. Accordingly, more detailed information about the EoR can be extracted from the cross-correlation, with less contamination from signals at lower redshift. Cross-correlation studies like these are also a way to confirm properties of the EoR inferred from each individual experiment.

LIM-21cm

LIM experiments provide an opportunity for creating datasets that are well-matched to 21cm observations from HERA and SKA. Unlike optical and near-IR experiments which will have a relatively narrow field of view, LIM observations promise widefield maps suitable for cross-correlations. Additionally, LIM techniques incorporate spectroscopic redshift information, which allows for meaningful comparison with 21 cm data which has had foreground cleaning or avoidance techniques applied. LIM-21 cm cross-correlations can help with constraining the properties of typical high-redshift galaxies, due to their ability to be used in inferring the size distribution of ionized regions during the EoR (Lidz et al., 2009, 2011).

21cm-CXB

Once the fluctuations in the CXB are measured they can be cross-correlated with the 21 cm measurements by experiments such as HERA

or the SKA. Properties of the first X-ray sources (including the bolometric luminosity, spectral energy distribution, spatial distribution of these sources and growth of the population in time) strongly affect predictions for the neutral hydrogen emission from redshifts $6 \lesssim z \lesssim 26$ with the exact range depending on model parameters. Cross-correlation between the CXB and the 21 cm signal is expected to be strong over the period when the 21 cm signal is driven by X-ray heating (e.g., Ma et al. 2018a). Moreover, the typical energy of produced radiation is imprinted in the shape of the cross-correlation. Thus, properties of typical high-redshift X-ray sources can be extracted from the CXB and the 21 cm signals.

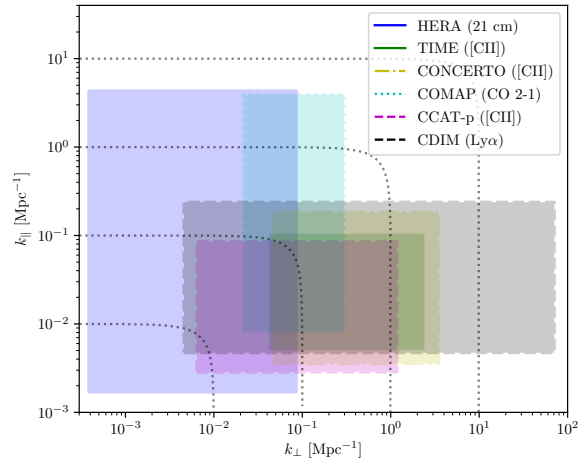


Figure 1: The overlap of various experiments in Fourier space as a function of comoving wavenumber in the plane of the sky (k_{\perp}) and along the line of sight (k_{\parallel}). Different boxes represent the rough coverage of various experiments. Not captured in the figure is the redshift overlap of the various experiments – in general, most of these cover the EoR and post-reionization epochs ($6 < z < 8$), which will provide for rich opportunities for cross-correlations.

Experiment	Tracer	Redshift	Angular Scales	Sky Coverage
HERA	21 cm	$5 < z < 25$	$11' < \theta < 120^\circ$	1440 deg^2
TIME	[CII]	$5 < z < 9$	$30'' < \theta < 1^\circ$	390 arcmin^2
CONCERTO	[CII]	$4.25 < z < 8.5$	$20'' < \theta < 1^\circ$	1.4 deg^2
COMAP	CO 2-1	$5.8 < z < 7.8$	$4' < \theta < 2^\circ$	5 deg^2
CCAT-p	[CII]	$3.25 < z < 9.25$	$1' < \theta < 8^\circ$	64 deg^2
CDIM*	Ly α	$6 < z < 8$	$1'' < \theta < 10^\circ$	100 deg^2
Simons Observatory	CMB	$z = 1100$	$1' < \theta < 8^\circ$	16500 deg^2
Lynx*	X-ray	$z \lesssim 10$	$0.3'' < \theta < 1^\circ$	1 deg^2
SKA-Low Phase 1	21 cm	$5 < z < 25$	$5' < \theta < 20^\circ$	100 deg^2

Table 1: A summary of the observational capabilities of several upcoming experiments which will make maps relevant to reionization physics. CDIM and Lynx are proposed experiments, and so the final observational strategies are not yet fixed.

The Road Ahead

While the science opportunities summarized above are potentially transformative significant challenges remain. Below we list our key recommendations for the coming decade. These recommendations focus on leveraging the full power of cross-correlations between maps generated by different experiments.

Recommendation 1: Promote Imaging Cross-correlation Studies

As a first step toward cross-correlation measurements, communication between the survey patterns and strategies for different experiments will be crucial for providing as much suitable data as possible. Beyond this, sharing data between experiments can be facilitated by the development of robust community-driven software libraries (e.g., Astropy Collaboration et al. 2018; Hazelton et al. 2017). Finally, efficient methods for generating maps and computing the statistical estimators required to extract the signal from these maps are an active and ongoing area of research. In particular, higher-point estimators such as the bispectrum and trispectrum can extract the non-Gaussian information present in the field. Other image-based methods can be used to implicitly leverage all non-Gaussian information present in maps (La Plante & Ntampaka, 2018).

Recommendation 2: Develop Self-Consistent Large-Scale Simulations

During cosmic dawn and the EoR, the detailed astrophysics of individual stars is indirectly coupled to the large scale observables in the IGM. Realistically and self-consistently modeling these tremendously different scales remains a theoretical challenge. Degeneracies in these physical models can be broken in principle by observations using different tracers, to get a more complete picture of the evolution of the Universe. Figure 1 and Table 1 sketch the coverage of Fourier modes, angular scales, and redshift ranges accessed by various current and planned experiments that will make maps of the EoR. These experiments will span many orders of magnitude, from proto-galaxy cluster scales (100 kpc) up to truly cosmological volumes (1 Gpc). Techniques for including predictions for the various physical tracers accurately for all scales of interest is highly non-trivial, as well as how to best incorporate observational artifacts of different experiments.

References

- Astropy Collaboration, Price-Whelan, A. M., Sipőcz, B. M., et al. 2018, *AJ*, 156, 123, doi: 10.3847/1538-3881/aabc4f
- Bosman, S. E. I., Fan, X., Jiang, L., et al. 2018, *MNRAS*, 479, 1055, doi: 10.1093/mnras/sty1344
- Bouwens, R. J., Illingworth, G. D., Oesch, P. A., et al. 2015, *ApJ*, 811, 140, doi: 10.1088/0004-637X/811/2/140
- Bowman, J. D., Rogers, A. E. E., Monsalve, R. A., Mozdzen, T. J., & Mahesh, N. 2018, *Nature*, 555, 67, doi: 10.1038/nature25792
- Burns, J. O., Nhan, B., Bradley, R. F., et al. 2018, in *American Astronomical Society Meeting Abstracts*, Vol. 232, *American Astronomical Society Meeting Abstracts #232*, 312.02
- Cappelluti, N., Ranalli, P., Roncarelli, M., et al. 2012, *MNRAS*, 427, 651, doi: 10.1111/j.1365-2966.2012.21867.x
- Cappelluti, N., Kashlinsky, A., Arendt, R. G., et al. 2013, *ApJ*, 769, 68, doi: 10.1088/0004-637X/769/1/68
- Cleary, K., Bigot-Sazy, M.-A., Chung, D., et al. 2016, in *American Astronomical Society Meeting Abstracts*, Vol. 227, *American Astronomical Society Meeting Abstracts #227*, 426.06
- Cohen, A., Fialkov, A., Barkana, R., & Lotem, M. 2017, *MNRAS*, 472, 1915, doi: 10.1093/mnras/stx2065
- Cooray, A., Bock, J., Burgarella, D., et al. 2016, *arXiv e-prints*, arXiv:1602.05178. <https://arxiv.org/abs/1602.05178>
- Crites, A. T., Bock, J. J., Bradford, C. M., et al. 2014, in *Society of Photo-Optical Instrumentation Engineers (SPIE) Conference Series*, Vol. 9153, *Millimeter, Submillimeter, and Far-Infrared Detectors and Instrumentation for Astronomy VII*, 91531W
- DeBoer, D. R., Parsons, A. R., Aguirre, J. E., et al. 2017, *PASP*, 129, 045001, doi: 10.1088/1538-3873/129/974/045001
- Dvorkin, C., Hu, W., & Smith, K. M. 2009, *Phys. Rev. D*, 79, 107302, doi: 10.1103/PhysRevD.79.107302
- Dvorkin, C., & Smith, K. M. 2009, *Phys. Rev. D*, 79, 043003, doi: 10.1103/PhysRevD.79.043003
- Fialkov, A., & Barkana, R. 2019, *arXiv e-prints*, arXiv:1902.02438. <https://arxiv.org/abs/1902.02438>
- Fialkov, A., Cohen, A., Barkana, R., & Silk, J. 2017, *MNRAS*, 464, 3498, doi: 10.1093/mnras/stw2540

- Gehlot, B. K., Koopmans, L. V. E., de Bruyn, A. G., et al. 2018, *MNRAS*, 478, 1484, doi: 10.1093/mnras/sty1095
- Hashimoto, T., Inoue, A. K., Mawatari, K., et al. 2018, arXiv e-prints, arXiv:1806.00486. <https://arxiv.org/abs/1806.00486>
- Hazelton, B. J., Jacobs, D. C., Pober, J. C., & Beardsley, A. P. 2017, *Journal of Open Source Software*, 2, 140:1, doi: <https://doi.org/10.21105/joss.00140>
- Keating, G. K., Marrone, D. P., Bower, G. C., et al. 2016, *ApJ*, 830, 34, doi: 10.3847/0004-637X/830/1/34
- Kovetz, E. D., Viero, M. P., Lidz, A., et al. 2017, arXiv e-prints, arXiv:1709.09066. <https://arxiv.org/abs/1709.09066>
- La Plante, P., & Ntampaka, M. 2018, arXiv e-prints, arXiv:1810.08211. <https://arxiv.org/abs/1810.08211>
- Lagache, G. 2017, *Proceedings of the International Astronomical Union*, 12, 228–233, doi: 10.1017/S1743921318000558
- Lehmer, B. D., Xue, Y. Q., Brandt, W. N., et al. 2012, *ApJ*, 752, 46, doi: 10.1088/0004-637X/752/1/46
- Lidz, A., Furlanetto, S. R., Oh, S. P., et al. 2011, *ApJ*, 741, 70, doi: 10.1088/0004-637X/741/2/70
- Lidz, A., Zahn, O., Furlanetto, S. R., et al. 2009, *ApJ*, 690, 252, doi: 10.1088/0004-637X/690/1/252
- Ma, Q., Ciardi, B., Eide, M. B., & Helgason, K. 2018a, *MNRAS*, 480, 26, doi: 10.1093/mnras/sty1806
- Ma, Q., Helgason, K., Komatsu, E., Ciardi, B., & Ferrara, A. 2018b, *MNRAS*, 476, 4025, doi: 10.1093/mnras/sty543
- Mitchell-Wynne, K., Cooray, A., Xue, Y., et al. 2016, *ApJ*, 832, 104, doi: 10.3847/0004-637X/832/2/104
- Monsalve, R. A., Greig, B., Bowman, J. D., et al. 2018, *ApJ*, 863, 11, doi: 10.3847/1538-4357/aace54
- Monsalve, R. A., Rogers, A. E. E., Bowman, J. D., & Mozdzen, T. J. 2017, *ApJ*, 847, 64, doi: 10.3847/1538-4357/aa88d1
- Moriwaki, K., Yoshida, N., Shimizu, I., et al. 2018, *MNRAS*, 481, L84, doi: 10.1093/mnras1/sly167
- Mortonson, M. J., & Hu, W. 2008, *ApJ*, 672, 737, doi: 10.1086/523958

- Parshley, S. C., Kronshage, J., Blair, J., et al. 2018, in Society of Photo-Optical Instrumentation Engineers (SPIE) Conference Series, Vol. 10700, Ground-based and Airborne Telescopes VII, 107005X
- Patil, A. H., Yatawatta, S., Koopmans, L. V. E., et al. 2017, *ApJ*, 838, 65, doi: 10.3847/1538-4357/aa63e7
- Roy, A., Lapi, A., Spergel, D., & Baccigalupi, C. 2018, *J. Cosmology Astropart. Phys.*, 5, 014, doi: 10.1088/1475-7516/2018/05/014
- Singh, S., Subrahmanyan, R., Udaya Shankar, N., et al. 2017, *ApJ*, 845, L12, doi: 10.3847/2041-8213/aa831b
- . 2018, *ApJ*, 858, 54, doi: 10.3847/1538-4357/aabae1
- The Lynx Team. 2018, arXiv e-prints, arXiv:1809.09642. <https://arxiv.org/abs/1809.09642>
- Venemans, B. P., Walter, F., Decarli, R., et al. 2017, *ApJ*, 851, L8, doi: 10.3847/2041-8213/aa943a